Striped networks and other hierarchical structures in $A_m B_m C_n$ $(2m+n)$-miktoarm star terpolymer melts

Jacob Judas Kain Kirkensgaard[*]

Department of Basic Sciences and Environment, Faculty of Life Sciences, University of Copenhagen, DK-1165 Copenhagen, Denmark

Using dissipative particle dynamics simulations we give numerical evidence of the formation of "striped" (or AB alternating) diamond and gyroid network structures and other hierarchical morphologies in $A_m B_m C_n$ $(2m+n)$-miktoarm star terpolymers where the main variable is the ratio $x = n/m$ with m,n being the number of equal length polymer arms of A and B and C, respectively. The formed networks are purely a result of the star topology, as clearly shown by direct comparison with parallel ABC miktoarm star terpolymer simulations with matching overall composition. Progressively changing x, the system adopts the following phase sequence: three-colored lamellae, C spheres embedded in AB lamellae, C spheres decorating AB lamellae, three-colored [6.6.6] tiling, AB striped diamond network, AB striped gyroid network, AB striped hexagonally arranged cylinders, and finally AB striped globular aggregates. The striped gyroid is particularly interesting as it constitutes an inherently chiral structure made from achiral building blocks.

I. INTRODUCTION

Recently the formation of a "striped" diamond or zinc-blende structure has been reported or predicted in various different but similar self-assembled soft matter systems. The first report was an experimental identification in a blend of ABC three-miktoarm star terpolymers and linear C homopolymers [1]. Later two simulation studies predicted the same structure in other related systems, one from self-assembled star polyphiles with unequal arm volumes [2] and one in a polymer-tethered nanoparticle system [3]. Among other things, this particular structure is interesting due to its potential as a self-organized photonic crystal where diamond-type structures are especially well suited because of their superior photonic band-gap properties [4]. In general, the self-assembly of new unusual morphologies is a growing field in contemporary soft matter research driven by the ability to synthesize increasingly complex molecular architectures [5]. Examples of recent complex ordered structures based on star-shaped molecules include (apart from the above mentioned) multicolored perforated lamellae [6], hierarchical lamellae [7], and novel network structures [8,9], all in various miktoarm star systems as well as a range of complicated cylindrical patterns in polyphilic bolaamphiphiles [10–13]. In this article, a conceptually simple road to obtain striped bicontinuous analog morphologies and other complex hierarchical structures is shown using computer simulations, and the importance of the molecular topology is emphasized as a way to control the interfacial curvature in liquid-crystalline soft matter assemblies. Ultimately we conclude that the molecular architecture should be considered as important a structural variable as composition and interaction parameters which in simpler linear copolymer systems are the overwhelmingly dominant characteristics.

The simulations presented here take their offspring in several numerical studies of three-armed ABC star molecules [14,15] where the main variable is the composition varied by

altering the length of the C arm while keeping the A and B arms the same size [see Fig. 1(b)]. Since two of the arms occupy the same volume, the compositional phase behavior is conveniently described as a function of a dimensionless parameter x defined as the volume ratio between the C arm and one of the A or B arms. The general consensus from this work is the formation of a number of cylindrical structures displaying a systematic progression through various two-dimensional tiling patterns as a function of x. Several of the predicted patterns from this work have been found in miktoarm star copolymer melts [8] and very recently also in much smaller intermediate molecular weight analogs, the above mentioned star polyphiles [16]. Many of the patterns found in these systems are a direct consequence of the molecular star architecture and likely impossible to form in normal linear copolymer systems. This stems mainly from the fact that, for sufficient segregation strength (which we assume to be the case here), the junctions of ABC stars have to assemble along lines compared to the junctions in linear AB or ABC systems which distribute on surfaces [17]. Ultimately this gives rise to a wealth of new possible structures.

To further illustrate the effect of molecular topology we here raise the complexity to another level and compare compositionally identical miktoarm star terpolymers distinguished only by the molecular connectivity. Specifically, we start from a symmetric ABC star molecule, i.e., a star with three mutually immiscible arms of equal length and with symmetric cross interactions between them. We then progressively add arms of the same length to change the composition, but to directly compare with previous work we again constrain two components to have the same size (here the same number of arms). This again makes it possible to quantify the composition by a single parameter, which is now defined as $x = n/m$ with m,n being the number of equal length A and B and C arms, respectively. Thus, to raise x we add C arms, and to lower x we add A and B arms. An example for $x = 2$ is shown in Fig. 1. For each step we compare the resulting morphology with the one obtained from the three-armed ABC star with matching composition, i.e., basically repeating the work mentioned

_____
[*]kirkensgaard@life.ku.dk
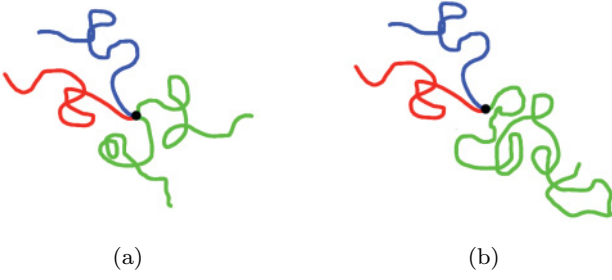
FIG. 1. (Color online) The topology of the miktoarm star copolymers investigated here. (a) An ABC_2 star. (b) The corresponding ABC star with matching composition. Both structures correspond to $x = 2$.

above as a reference for direct comparison. The results presented here can be seen as a subset of a more general exploration of $A_l B_m C_n$ miktoarm star copolymers here with $l = m$. The vastly more exhaustive numerical investigation of the (l,m,n) parameter space in this polymer system will be published elsewhere.

II. SIMULATION DETAILS

The self-assemblies of the different miktoarm stars are investigated using dissipative particle dynamics (DPD) simulations where the molecular topology is built up by connecting particles (or beads) appropriately. The time evolution of an ensemble of DPD particles is found by solving Newton's equations of motion. The ith particle experiences a pairwise additive force with a conservative, a dissipative, and a random component:

$$\mathbf{F}_{ij} = \sum_{i \neq j} \mathbf{F}_{ij}^C + \mathbf{F}_{ij}^D + \mathbf{F}_{ij}^R, \tag{1}$$

with the sum running over all j particles within a cutoff radius $r_c = 1$. The reduced DPD units are defined as $r_c = m = k_B T = 1$ and thus $t = r_c(m/k_B T)^{\frac{1}{2}}$. The DPD conservative force used derives from the soft potential:

$$V^C(r_{ij}) = \begin{cases} \frac{a_{ij}}{2}\left(1 - \frac{r_{ij}}{r_c}\right)^2 & \text{for} \quad r_{ij} \leqslant r_c, \\ 0 & \text{for} \quad r_{ij} > r_c \end{cases} \tag{2}$$

where a_{ij} and r_{ij} are the interaction parameter and distance between particles i and j, respectively. This potential leads to a conservative force:

$$\mathbf{F}^C(r_{ij}) = a_{ij} \sum_j f_c(r_{ij}) \hat{\mathbf{r}}_{ij}, \tag{3}$$

with

$$f_c(r_{ij}) = \begin{cases} 1 - \frac{r_{ij}}{r_c} & \text{for} \quad r_{ij} \leqslant r_c, \\ 0 & \text{for} \quad r_{ij} > r_c \end{cases} \tag{4}$$

and $\hat{\mathbf{r}}_{ij}$ denoting a unit vector between the two particles.

The dissipative force is a hydrodynamic drag (or friction) force depending on the velocity $\mathbf{v}_{ij}$ between particles i and j and given by

$$\mathbf{F}^D(r_{ij}) = \begin{cases} -\gamma \omega^D(r_{ij})(\hat{\mathbf{r}}_{ij} \cdot \mathbf{v}_{ij})\hat{\mathbf{r}}_{ij} & \text{for} \quad r_{ij} \leqslant r_c \\ 0 & \text{for} \quad r_{ij} > r_c \end{cases}. \tag{5}$$

Here γ is the friction coefficient setting the strength of the dissipative force and ω^D is a weight function defined below. The random force is

$$\mathbf{F}^R(r_{ij}) = \sigma \omega^R(r_{ij}) \frac{\theta_{ij}}{\sqrt{\Delta t}} \hat{\mathbf{r}}_{ij}. \tag{6}$$

Again ω^R is a weight function, σ is the strength of the random force, Δt is a time step in the integration algorithm, and θ_{ij} is a Gaussian distributed random variable different for each particle pair and without memory (i.e., it changes after each time step). The random force mimics a thermal noise and together with the friction force acts as a thermostat (as a heat source and sink, respectively). The weight functions and constants from the dissipative and random forces are related by

$$\sigma^2 = 2\gamma k_B T \tag{7}$$

and

$$\omega^D = [\omega^R]^2, \tag{8}$$

ensuring that the fluctuation-dissipation theorem is satisfied [18] and with the weight function usually taken as

$$\omega^D = \begin{cases} (r_c - r_{ij})^2 & \text{for} \quad r_{ij} \leqslant r_c \\ 0 & \text{for} \quad r_{ij} > r_c \end{cases}. \tag{9}$$

Connected beads in each molecule are held together by harmonic bonds:

$$V^B = \frac{C}{2}(r_{ij} - r_0)^2, \tag{10}$$

with $r_0 = 0$ and $C = 4$. The integration of the equations of motion is done using a standard velocity-Verlet algorithm with time step $\Delta t = 0.02$. Other parameters relevant for the DPD implementation [19] are $\gamma = 4.5$ and thus $\sigma = 3$. All simulations are performed in a cubic box of volume L^3 and with particle density $\rho = 3$. Thus, the number of particles in each simulation is $3L^3$. The majority of the simulations are done with $L = 20$, but all presented results have been checked for finite-size effects from the simulation box by simulating in different box sizes in the range 18 to 22. At a density of $\rho = 3$ the interaction parameter between unlike particles can be related to the Flory-Huggins interaction parameter χ_{ij} [20] so that

$$a_{ij} = a_{ii} + 3.497\chi_{ij}, \tag{11}$$

with the like-like interaction parameter being determined from the compressibility of water to be

$$a_{ii} = 75k_B T/\rho = 25 \tag{12}$$

for $\rho = 3$. Here we set $a_{ij} = 36$, which has previously been shown to be a good value to represent a nicely segregated system with reasonable simulation times to reach equilibrated structures [19]. For the $A_m B_m C_n$ $(2m + n)$-miktoarm stars each arm is made of four beads; thus each molecule contains $N = 1 + 4(2m + n)$ beads. The ABC stars directly match the composition at each value of $x = n/m$, only distributed on three chains as illustrated in Fig. 1. Details about the exact number of beads representing each investigated molecule are listed in Tables I and II for the ABC three-miktoarm stars and $A_m B_m C_n$ $(2m + n)$-miktoarm stars, respectively. Simulations

TABLE I. Simulation details for ABC three-miktoarm star terpolymers. The columns list x, number of beads in each arm (A and B are always the same), and the resulting morphology.

x	No. A beads	No. C beads	Morphology
0.25	8	2	[LAM$_3$]
0.33	9	3	[LAM$_3$]
0.5	8	4	[8.8.4]
1	4	4	[6.6.6]
2	4	8	[10.6.4;10.6.6]
3	4	12	[ALT LAM]
4	4	16	[ALT LAM]
5	4	20	[ALT LAM]
6	3	18	[ALT LAM]
8	2	16	[ALT PL]
8	3	24	[ALT PL]
10	2	20	[ALT CYL]

were run using the ESPResSo package [21] and simulation snapshots were all made with the VMD package [22].

III. RESULTS

In Fig. 2 our results are summarized by a direct comparison of the two star variants. For $x = 1$ the two situations are identical and the resulting morphology of this balanced ABC star is the so-called three-colored hexagonal honeycomb following the [6.6.6] tiling. We have checked the self-assembly of $x = 1$ stars for up to five arms ($m = n = 5$) of each color and the [6.6.6] structure persists for all investigated cases. This structure is also found in all the previously mentioned simulation investigations of these molecules as well as in several of the

TABLE II. Simulation details for $A_m B_m C_n$ $(2m + n)$-miktoarm star terpolymers. The columns list x, the number of arms of equal length (A and B are always the same), and the resulting morphology.

x	No. A arms	No. C arms	Morphology
0.25	4	1	[LAM$_3$]
0.33	3	1	[S in LAM]
0.5	2	1	[DEC LAM]
0.5	4	2	[DEC LAM]
0.67	3	2	[6.6.6]
0.75	4	3	[6.6.6]
1	1	1	[6.6.6]
1	2	2	[6.6.6]
1	3	3	[6.6.6]
1	4	4	[6.6.6]
1	5	5	[6.6.6]
1.33	3	4	[6.6.6]
1.5	2	3	[6.6.6]
2	1	2	[ALT D]
2	2	4	[ALT D]
3	1	3	[ALT G]
4	1	4	[ALT CYL]
5	1	5	[ALT CYL]
6	1	6	[ALT CYL]
8	1	8	[ALT CYL]
10	1	10	[S$_{AB}$]

experimental papers. Starting with the progression of phases for the reference simulations of the ABC three-miktoarm stars shown below the x axis in Fig. 2, we find excellent agreement with previous studies of this system [14,15,23,24]. In summary, at low x a lamellar structure is formed with the minority component distributed on the dividing interface between the two majority components. For $0.33 < x < 3$ a number of tiling patterns are formed with the polygonal composition changing systematically to accommodate the changing volume fraction in the systems. The phase progression goes as [8.8.4] → [6.6.6] → [10.6.4;10.6.6] for increasing x. Had we investigated with a finer compositional resolution we would probably have found two other tilings usually also found in these systems, the [8.6.4;8.6.6] and [12.6.4] tilings, respectively. This is thoroughly documented in the references given above. For $3 \leqslant x \leqslant 6$ a hierarchical lamellar structure denoted [ALT LAM] appears where the majority component forms lamellae in one direction divided by a layer of alternating minority components forming a shorter spaced lamellar structure perpendicular to the first. At $x = 8$ we have difficulty stabilizing a single ordered structure but find either an unordered network or a perforated lamellae structure of alternating minority components in a matrix of the green majority component. This marks the transition to a regime of cylindrical structures starting at $x = 10$ where the minority components form alternating AB cylinders in a matrix of C. This is all in perfect agreement with the results from [14], also the difficulty in establishing any definite ordered structure around $x = 8$. We have not investigated higher values of x as the simulations become progressively time-consuming for higher x but this regime has been documented in the above cited work and the results suggest that the [ALT CYL] structure persists to around $x = 18$, after which spherical AB aggregates with internal lamellar structure are formed in a matrix of the C component [14].

As we turn to the $A_m B_m C_n$ system a completely different phase progression appears, shown above the x axis in Fig. 2. The most remarkable difference between the two scenarios is when going from $x = 1$ to 4. Here the altered molecular architecture results in a distinct phase progression going from the [6.6.6] tiling → [ALT D] (striped diamond) → [ALT G] (striped gyroid) → [ALT CYL] (striped cylinders). In Figs. 3 and 4 more detailed views are shown of the two striped network structures [ALT D] and [ALT G]. Note that by fusing the minority components we would in both these cases recover the usual bicontinuous diamond and gyroid structures found ubiquitously in synthetic and natural soft matter systems [25]. In the bicontinuous gyroid, the two intertwined networks are chiral enantiomers (left- and right-handed *srs* nets, respectively) [26], thus the [ALT G] morphology is inherently chiral since one net is now split into two components. Comparing directly with the ABC three-miktoarm stars, we see that the induced curvature stemming from the increased number of arms dramatically alters the relative composition needed to form the [ALT CYL] structure which first appears for $x = 4$ and 10 in the two cases, respectively. This could have important consequences in the design of specific material properties, for example thermoplastic elastomers. For $x < 1$ the phase progression is also altered. We still find a [LAM$_3$] structure at $x = 0.25$, but then two new lamellar structures are found with
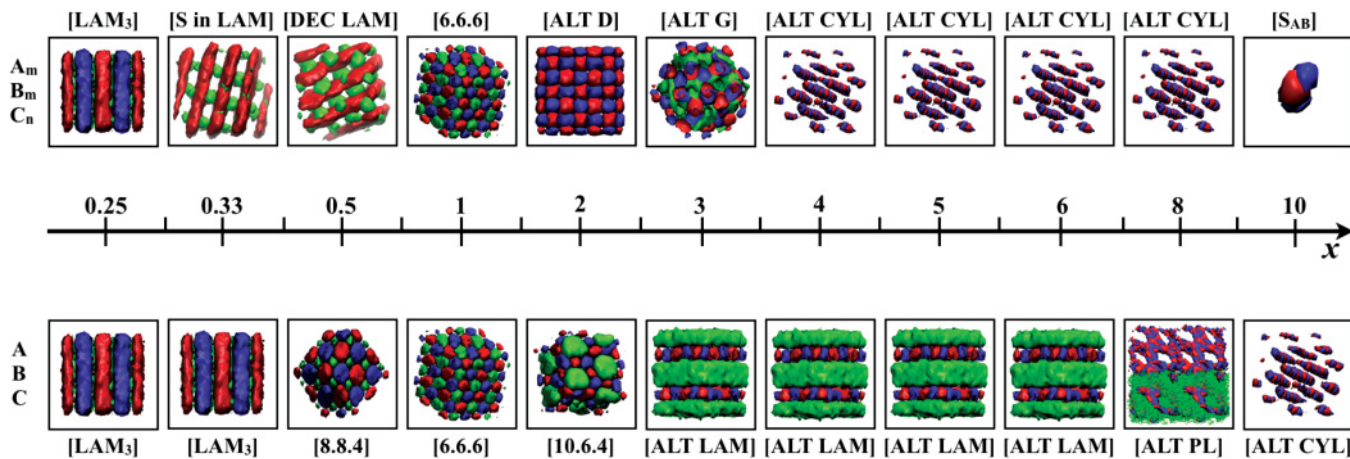
FIG. 2. (Color online) Overview of the morphologies obtained when varying x, the number of arms in an $A_m B_m C_n$ star miktoarm terpolymer with $x = n/m$ (top row), and the corresponding morphologies in an ABC three-miktoarm star system with equal composition (bottom row). The tiling patterns are labeled by their Schläfli symbol [14] assigned by looking at the polygonal composition around a tiling vertex.

the minority components forming globular aggregates. First at $x = 0.33$ each minority component globule is embedded within one of the two lamellar majority components, denoted [S in LAM] in Fig. 2. At $x = 0.5$ the globules are distributed on the lamellar AB interface so that each globule has half its volume inside each majority domain, thus decorating the interface, denoted [DEC LAM] in Fig. 2. In both cases the in-plane globule packing is hexagonal.

It is clear from Fig. 2 that the molecular connectivity is vital for the resulting self-assembly morphology and effectively can be considered an additional variable together with composition and interactions. As mentioned initially, an [ALT DIA] structure was found experimentally in a blend system where an ABC star was swelled by selective addition of C homopolymer chains [1]. In that particular polymer system, the
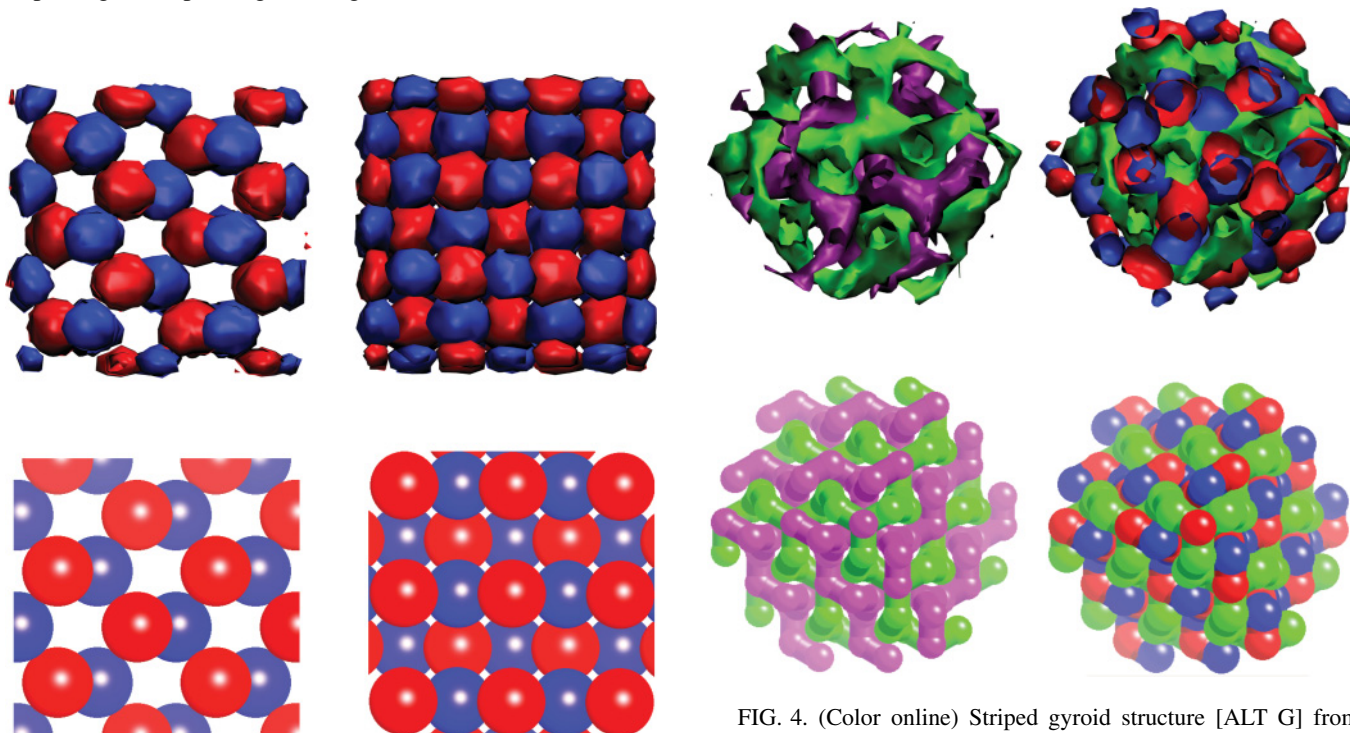

FIG. 3. (Color online) Striped diamond (or zinc-blende) structure [ALT D] from ABC_2 miktoarm star ($x = 2$) with symmetry $F\bar{4}3m$. Each globular domain of red (light gray) [blue (dark gray)] is tetragonally connected to four blue (dark gray) [red (light gray)] globular domains building up a diamond network. Here views along the [011] (left) and [010] (right) directions are shown from the simulation (top) and crystallographic model (bottom). The green component is not shown for better visualization.

FIG. 4. (Color online) Striped gyroid structure [ALT G] from ABC_3 miktoarm star ($x = 3$) with symmetry $P4_132$. This structure is chiral. All views are along the [111] showing the simulation (top) and crystallographic model (bottom). On the left the red and blue components have been fused [shown in purple (dark gray)], illustrating that they together form a single srs net as does the majority component [green component (lightest gray) in all four images]. On the right we see that each globular domain of red (light gray) [blue (dark gray)] is connected to three blue (dark gray) [red (light gray)] globular domains building up the single gyroidal network.

interaction parameters were far from symmetric, though, and the increased surface tension between one pair of components effectively acted to induce the interfacial curvature which in the simulations presented here resulted from the molecular architecture. The combined effect of these variables remains to be explored in the present system.

IV. CONCLUDING REMARKS

By simply changing the number of equal length polymer arms in a three component terpolymer star system, we have demonstrated a dramatic effect of the molecular architecture on the resulting self-assembly morphologies resulting in a new phase progression as compared to simpler ABC three-miktoarm stars with matching composition and cross interactions. In particular, the easy formation of new complicated striped network structures with potential applications in, for example, photonics is interesting. As a final note, it should be emphasized that the forefront of modern polymer chemistry capabilities now allows the synthesis of multicomponent asymmetric star polymers including several $A_l B_m C_n$ architectures, as has been investigated in this study [27]. However, no detailed morphological studies have been presented of these molecules yet. The results presented here make us anticipate that a number of interesting structures can be found in these novel polymer systems, and we await experimental verification of this.

[1] K. Hayashida, A. Takano, T. Dotera, and Y. Matsushita, Macromolecules **41**, 6269 (2008).

[2] J. J. K. Kirkensgaard and S. Hyde, Phys. Chem. Chem. Phys. **11**, 2016 (2009).

[3] C. Iacovella and S. C. Glotzer, Nano Lett. **9**, 1206 (2009).

[4] M. Maldovan and E. Thomas, Nat. Mater. **3**, 593 (2004).

[5] T. Higashihara, K. Sugiyama, H. Yoo, M. Hayashi, and A. Hirao, Macromolecular Rapid Communications **31**, 1031 (2010).

[6] J. J. K. Kirkensgaard, P. Fragouli, N. Hadjichristidis, and K. Mortensen, Macromolecules **44**, 575 (2011).

[7] Y. Matsushita, A. Takano, K. Hayashida, T. Asari, and A. Noro, Polymer **50**, 2191 (2009).

[8] Y. Matsushita, K. Hayashida, T. Dotera, and A. Takano, J. Phys. Condens. Matter **23**, 284111 (2011).

[9] J. J. K. Kirkensgaard, *Interface Focus* (2012).

[10] C. Tschierske, C. Nürnberger, H. Ebert, B. Glettner, M. Prehm, F. Liu, X.-B. Zeng, and G. Ungar, *Interface Focus* (2012).

[11] G. Ungar, C. Tschiersk, V. Abetz, R. Holyst, B. M., F. Liu, M. Prehm, R. Kieffer, X. Zeng, W. M., B. Glettner, and A. Zywocinski, Adv. Funct. Mater. **21**, 1296 (2011).

[12] A. Crane, F. Martinez-Veracoechea, F. Escobedo, and E. Müller, Soft Matter **4**, 1820 (2008).

[13] A. Crane and E. Müller, Faraday Discuss. **144**, 187 (2010).

[14] T. Gemma, A. Hatano, and T. Dotera, Macromolecules **35**, 3225 (2002).

[15] C.-I. Huang, H.-K. Fang, and C.-H. Lin, Phys. Rev. E **77**, 031804 (2008).

[16] L. de Campo, T. Varslot, M. Moghaddam, J. Kirkensgaard, K. Mortensen, and S. Hyde, Phys. Chem. Chem. Phys. **13**, 3139 (2011).

[17] S. T. Hyde, L. de Campo, and C. Oguey, Soft Matter **5**, 2782 (2009).

[18] P. Espanol and P. Warren, Europhys. Lett. **30**, 191 (1995).

[19] J. J. K. Kirkensgaard, Soft Matter **6**, 6102 (2010).

[20] R. Groot and P. Warren, J. Chem. Phys. **107**, 4423 (1997).

[21] H. J. Limbach, A. Arnold, B. A. Mann, and C. Holm, Comput. Phys. Commun. **174**, 704 (2006).

[22] W. Humphrey, A. Dalke, and K. Schulten, J. Mol. Graphics **14**, 33 (1996).

[23] W. Li, Y. Xu, G. Zhang, F. Qiu, Y. Yang, and A. Shi, J. Chem. Phys. **133**, 064904 (2010).

[24] J. J. K. Kirkensgaard, Soft Matter **7**, 10756 (2011).

[25] S. Hyde, S. Andersson, Z. Blum, S. Lidin, K. Larsson, T. Landh, and B. Ninham, *The Language of Shape* (Elsevier, Amsterdam, 1997).

[26] M. O'Keeffe, M. A. Peskov, S. J. Ramsden, and O. M. Yaghi, Acc. Chem. Res. **41**(12), 1782 (2008).

[27] T. Higashihara, T. Sakurai, and A. Hirao, Macromolecules **42**, 6006 (2009).